Unusual 180° P−O−P Bond Angles in ZrP_2O_7

N. Khosrovani, V. Korthuis, and A. W. Sleight*

Department of Chemistry, Oregon State University, Corvallis, Oregon 97331-4003

T. Vogt

Physics Department, Brookhaven National Laboratory, Upton, Long Island, New York 11973

Received July 7, 1995[⊗]

The structure of cubic ZrP_2O_7 at room temperature has been solved and refined using a combination of modeling and high-resolution neutron powder diffraction data. The cell edge is 24.74 Å, the space group is $Pa\bar{3}$, and Z is 108. For those P_2O_7 units not on a 3-fold axis, the P−O−P angles range from 134° to 162°. Two crystallographically distinct P_2O_7 groups are on three fold axes with P−O−P angles thus constrained to be 180° on average. The structure of cubic ZrP_2O_7 was also refined from data taken at 227, 290, 371, 435, and 610 °C. The $3 \times 3 \times 3$ superstructure present at room temperature disappears at about 290 °C, and all P−O−P angles of P_2O_7 are then constrained by symmetry to be 180° on average. The exceptionally low thermal expansion shown by ZrP_2O_7 above 290 °C is likely related to the unusual P−O−P angle.

Introduction

A cubic structure is found for phosphates of the type $A^{4+}P_2O_7$, where A^{4+} may be Si, Ge, Sn, Pb, Ti, Zr, Hf, Mo, W, Re, Ce, Th, U, or Pu.[1−13] Double substitution on the A site leads to a series of the type $A^{3+}_{0.5}A^{5+}_{5.5}P_2O_7$, where A^{3+} may be Bi, Sb, or a rare earth and A^{5+} may be Nb, Ta, or Sb.[14] One form of $Sb^{3+}Sb^{5+}(P_2O_7)_2$ also has a closely related structure.[15] Arsenates are reported with this structure for A^{4+} = Zr or Th,[16,17] and vanadates are reported for A^{4+} = Zr or Hf.[18−21]

This cubic AM_2O_7 structure where M may be P, As, or V can be viewed as related to the NaCl structure. The cation is A^{4+}, and the anion is $(M_2O_7)^{4-}$. The ordered orientation of the $(M_2O_7)^{4-}$ group necessarily lowers the symmetry; the highest symmetry possible for this framework (Figure 1) is $Pa\bar{3}$. In this ideal structure with $Z = 4$, the M_2O_7 group is on a 3-fold axis with the bridging oxygen on an inversion center. The M−O−M bond angle is, therefore, constrained to be 180° on average. At high temperature, it appears that all compounds in this structure type can be described in this $Pa\bar{3}$ space group with $Z = 4$. However, some, and perhaps all, of these cubic AM_2O_7 compounds undergo a phase transition with decreasing temperature. It appears that the low-temperature structure remains cubic with the same space group but with a $3 \times 3 \times 3$ superstructure. Only in the case of SiP_2O_7 has a solution to this superstructure been reported.[22]

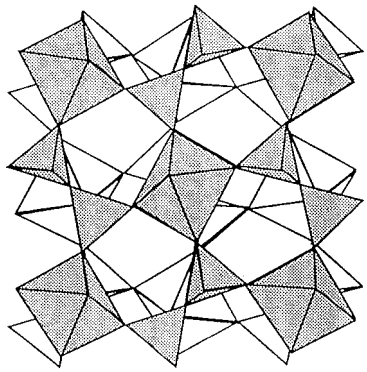

Figure 1. Ideal structure for cubic AM_2O_7 compounds shown as corner sharing AO_6 octahedra and MO_4 tetrahedra.

The thermal expansion of cubic AM_2O_7 phases can be very low and even negative in the temperature range where there is no superstructure. In the case of ZrP_2O_7, the thermal expansion might be considered normal from room temperature to about 290 °C. The superstructure disappears at this temperature, and the thermal expansion from 290 to 610 °C is about 3.5×10^{-6} $°C^{-1}$, which is very low.[21,23,24] The thermal expansion actually becomes negative in the cases of ThP_2O_7, UP_2O_7, ZrV_2O_7, and HfV_2O_7.[19−21,23]

[⊗] Abstract published in *Advance ACS Abstracts,* December 15, 1995.

(1) Laud, K. R.; Hummel, R. A. *J. Am. Ceram. Soc.* **1971**, *54*, 296.
(2) Harrison, D. E.; Hummel, R. A. *J. Am. Ceram. Soc.* **1959**, *42*, 487.
(3) Merz, K. M.; Smyth, H. T.; Kirchner, H. P.; Beal, J. L. Report No. PI−1273−M−8; Cornell Aeronautical Laboratory, 1960.
(4) Harrison, D. E.; McKinstry, H. A.; Hummel, F. A. *J. Am. Ceram. Soc.* **1954**, *37*, 277.
(5) Burdese, A.; Lucco Borlera, M. *Ann Chim. (Rome)* **1963**, *53*, 333.
(6) Burdese, A.; Lucco Borlera, M. *Atti. Accad. Sci. Torino, Cl. Sci. Fis., Mater. Nat.* **1959**, *94*, 107.
(7) Huang, C.−H.; Knop, O.; Othen, D. A. *Can. J. Chem*. **1975**, *53*, 79.
(8) Völlenkle, H.; Wittman, A.; Nowotny, H. *Monatsh. Chem.* **1963**, *94*, 956.
(9) Hagman, L.−O.; Kierkegaard, P. *Acta Chem. Scand.* **1969**, *23*, 327.
(10) Liebau, F.; Bissert, G.; Koppen, N. *Z. Anorg. Allg. Chem.* **1968**, *359*, 113.
(11) Kinomura, N.; Hirose, M.; Kumada, N.; Muto, F. *Mater. Res. Bull.* **1985**, *20*, 379.
(12) Bjorklund, C. W. *J. Am. Chem. Soc.* **1957**, *79*, 6347.
(13) Teweldemedhin, Z. S.; Ramanujachary, K. V.; Greenblatt, M. *Mater. Res. Bull*. **1993**, *28*, 427.
(14) Oyetola, S.; Verbaere, A.; Guyomard, D.; Crosnier, M. P.; Piffard, Y.; Tournoux, M. *Eur. J. Solid State Inorg. Chem.* **1991**, *28*, 23.
(15) Verbaere, A.; Oyetola, S.; Guyomard, D.; Piffard, Y. *J. Solid State Chem.* **1988**, *75*, 217.
(16) Hajo, O. *Naturwissenschaften* **1965**, *52*, 344.
(17) Le Flem, G.; Lamic, J.; Hagenmulller, P. *Mémoires Présentés A La Société Chimique,* June 1966; p 1880.
(18) Peyronel, G. *Gazz. Chim. Ital.* **1942**, *72*, 77.
(19) Craig, D. F.; Hummel, F. A. *J. Am. Ceram. Soc.* **1972**, *55*, 532.
(20) Buchanan, R. C.; Wolter, G. W. *J. Electrochem. Soc.* **1983**, *130*, 1905.
(21) Korthuis, V.; Khosrovani, N.; Sleight, A. W. *Chem. Mater*. **1995**, *7*, 412.
(22) Tillmanns, E.; Gebert, W.; Baur, W. H. *J. Solid State Chem*. **1973**, *7*, 69.
(23) Taylor, D. *Br. Ceram. Trans. J.* **1984**, *83*, 129.

0020-1669/96/1335-0485$12.00/0

Table 1. Cell Parameters and Agreement Factors at Different Temperatures

	290 °C	371 °C	435 °C	610 °C
a (Å)[a]	8.2899(1)	8.2928(1)	8.2953(1)	8.2991(1)
R_{wp}	0.0677	0.0644	0.0693	0.0817
R_{calc}	0.0564	0.0505	0.0584	0.0772
$R(F^2)$	0.0733	0.0640	0.0633	0.1024
χ^2	0.6216	0.5605	0.6899	2.464

[a] Standard deviations in parentheses are those calculated by GSAS. Considering the uncertainties in the wavelength and temperature, the uncertainty of the cell edges would be much larger.

Our primary motivation in studying ZrP_2O_7 was to understand the unusual thermal expansion properties that can occur for the cubic AM_2O_7 compounds. Secondly, we were interested in the challenge of accounting for a $3 \times 3 \times 3$ superstructure using powder diffraction data.

Experimental Section

Our synthesis procedure for ZrP_2O_7 has been previously reported.[21,24] Diffraction data were obtained on the high-resolution neutron powder diffractometer at beam line H1A of the high-flux beam reactor at Brookhaven National Laboratory.[25]

The high-temperature data were collected using a furnace with resistive heaters and aluminum heat shields. The sample was pressed into a cylindrical pellet 3 cm high and 1 cm in diameter. Two stainless steel coated thermocouples, one above and one below the sample, were used to monitor the temperature. The sample was exposed to air during data collection, which did not commence until thermal equilibrium was achieved.

Results

High-Temperature Structure. No superstructure was observed in data collected at 290, 371, 435, and 610 °C. Therefore, these data were refined using space group $Pa\bar{3}$ with $Z = 4$. The cell edges and agreement factors are given in Table 1, and an example of an observed and calculated pattern is given in Figure 2. The variation with temperature of these cell edges is in good agreement with the thermal expansion data for ZrP_2O_7 reported by us[21,24] and by others.[23] All of the data collected above room temperature contained peaks of aluminum due to the heat shields. Thus, all refinements of such data were two-phase refinements. The higher values of agreement factors at 610 °C (Table 1) can be attributed to poorer statistics resulting from a furnace configuration necessitated by the higher temperature. The standard deviations of refined parameters are not much increased (Table 2) for the 610 °C data.

The refined parameters for high-temperature ZrP_2O_7 are given in Table 2. Zirconium and O2 are at special positions (0, 0, 0) and (0.5, 0.5, 0.5), respectively. A good fit to the data required the use of anisotropic thermal parameters for both O1 and O2. These oxygen atoms show thermal vibration primarily perpendicular to the bond: Zr−O1−P or P−O2−P (Figure 3). The vibration of O2 is unusually large. Consequently, O2 was also modeled with a static displacement by placing one-sixth of an atom in the general position. This led to an essentially equivalent fit to the data.

Some interatomic distances and angles are given in Table 3. Over this 320 °C temperature range, there are only minor changes in positional parameters or interatomic distances.

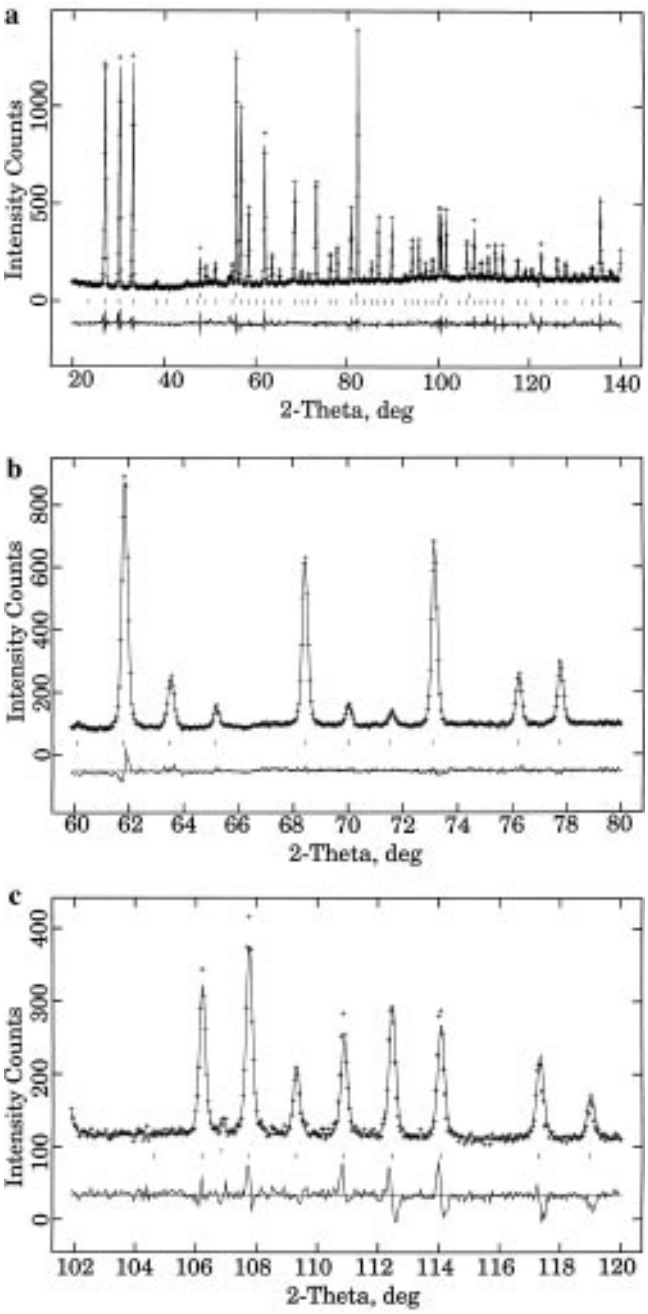

Figure 2. Observed (crosses) and calculated (line) neutron diffraction patterns for ZrP_2O_7 at 371 °C: (a) 2-θ range 20−140°. (b) 2-θ range 60−80°. (c) 2-θ range 102−120°. The upper ticks are due to aluminum in the furnace; the lower pattern is the difference between observed and calculated intensity.

Low-Temperature Structure. A structural solution based on data taken at 227 °C and room temperature is highly challenging. The fact that the space group remains $Pa\bar{3}$ is confirmed by ^{31}P NMR studies.[21] However, Z is now 108 due to the $3 \times 3 \times 3$ superstructure. There are 134 positional parameters for about 2600 possible peaks in the range of the data collection. An attempt was made to refine the ZrP_2O_7 neutron diffraction data using as starting parameters the published atomic coordinates for SiP_2O_7.[22] This and similar approaches always led to convergence with highly unreasonable interatomic distances. We therefore resorted to modeling as was also done in the case of SiP_2O_7.[22]

The distance-least-squares approach to modeling was employed.[26] In this approach, the ZrO_6 octahedron and PO_4

(24) Mary, T. A.; Korthuis, V.; Khosrovani, N.; Sleight, A. W. In *Low-Expansion Materials, Ceramic Transactions*, Vol. 52; Stinton, D. P., Limaye, S. Y., Eds.; American Ceramic Society: Westerville, OH, 1995; pp 81−87.

(25) Buttrey, D. J.; Vogt, T; Wildgruber, U.; Robinson, W. R. *J. Solid State Chem.* **1994**, *111*, 118.

(26) Meier, W. M.; Villiger, H. *Z. Kristallogr.* **1966**, *129*, 161.

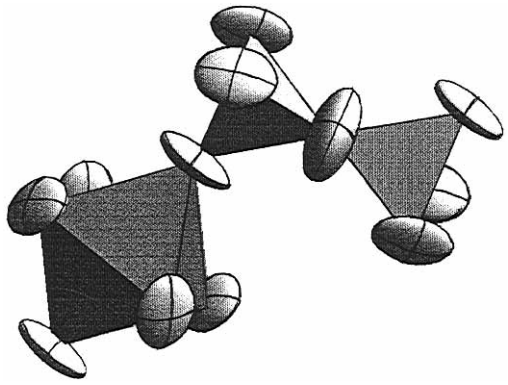

Figure 3. Phosphate tetrahedra and a zirconium octahedron showing the thermal ellipsoids for ZrP_2O_7 at 25 °C.

Table 2. Fractional Coordinates and Thermal Parameters at Different Temperatures with Standard Deviations in Parentheses

atom		290 °C	371 °C	435 °C	610 °C
Zr	*x*	0	0	0	0
	U(iso)	0.0210(6)	0.0203(6)	0.0236(7)	0.0242(7)
P	*x*	0.3946(3)	0.3947(2)	0.3949(3)	0.3940(3)
	U(iso)	0.0217(8)	0.0218 (8)	0.0232(8)	0.0227(9)
O1	*x*	0.4450(2)	0.4448(2)	0.4444(3)	0.4446(3)
	y	0.2267(2)	0.2269(2)	0.2265(2)	0.2263(2)
	z	0.4240(3)	0.4234(3)	0.4234(3)	0.4235(4)
	*U*11	0.0771(21)	0.0793(21)	0.0829(22)	0.0826(26)
	*U*22	0.0282 (13)	0.0258 (12)	0.0287 (13)	0.0324 (16)
	*U*33	0.0947(21)	0.0903(19)	0.0939(21)	0.0970(26)
	*U*12	0.0214(12)	0.0240(12)	0.0225(13)	0.0253(16)
	*U*13	0.0205(13)	0.0187(13)	0.0198(14)	0.0146(18)
	*U*23	0.0291(15)	0.0290(14)	0.0270(15)	0.0250(20)
O2	*x*	0.5	0.5	0.5	0.5
	*U*11[a]	0.1355(34)	0.1333(32)	0.1337(34)	0.1371(44)
	*U*12[a]	−0.0500(38)	−0.0491(37)	−0.0478(40)	−0.0517(49)

[a] $U11 = U22 = U33$; $U12 = U13 = U23$.

Table 3. Selected Interatomic Distances (Å) and Angles (deg) at Different Temperatures

	290 °C	371 °C	435 °C	610 °C
P−O1	1.474(2)	1.472(2)	1.475(2)	1.474(2)
P−O2	1.514(4)	1.513(4)	1.510(4)	1.524(4)
P−O2[a]	1.520	1.519	1.516	1.530
Zr−O1	2.034(2)	2.038(2)	2.036(2)	2.035(2)
Zr−O1−P	171.0(2)	170.7(2)	170.7(2)	170.9(2)

[a] This distance is corrected for the thermal motion of O2.

tetrahedron are semirigid, but O−Zr−O and O−P−O angles are less restrained than Zr−O and P−O distances. The Zr−O−P and P−O−P linkages are considered to be highly flexible, but cation−cation distances are not allowed to be unreasonably short. The *R* value in this least-squares refinement is defined as $R = \sum(w\delta d)^2/\sum(wd)^2)^{1/2}$, where *d* is a Zr−O, P−O, or O−O distance, δd is the difference between the prescribed and actual distances, and *w* is a weighting factor. The prescribed weights in our modeling are as follows: 2.00 for Zr−O and P−O distances, 0.25 for O−O distances, 0.25 for P−P distances, and 0.001 for Zr−P distances. Different P−O distances were prescribed depending on whether or not a particular P−O−P linkage was on a 3-fold axis. For those P−O−P linkages not on a 3-fold axis, normal P−O distances were prescribed. However, for a P−O−P linkage on a 3-fold axis, the prescribed P−O distance was shortened to reflect the assumption that this P−O−P linkage was in reality bent in a normal, but disordered, way. Refinements initiated with different sets of random numbers were used to assure that the global minimum was obtained. The *R* value obtained for the $3 \times 3 \times 3$ superstructure is 2.0% in space group $Pa\bar{3}$. The final coordinates from this refinement are used as the starting model for the GSAS[27] program. The profile function used for the 25 °C refinement is the standard Gaussian modified for peak asymmetry,[27,28] and the profile function used for the 227 °C refinement is the pseudo-Voigt.[29] The background function used in both 25 and 227 °C refinements is the Chebyschev polynomial of the first kind with five coefficients. The P−O−P bridging oxygen atoms not on the 3-fold axis (O1−O4) are constrained to have equal isotropic thermal parameters, whereas the P−O−P bridging oxygen atoms on the 3-fold axis are refined with anisotropic thermal parameters (O5−O6). All of the oxygen atoms in the Zr−O−P linkages are constrained to have equal isotropic thermal parameters (O7−O33). Additional constraints are used to avoid local minima with unreasonable distances. A low *R* value is easily obtained with a poor fit to the superstructure peaks. Thus, our strategy was to focus on obtaining a good fit to the superstructure peaks, which was in fact achieved (Figure 4). Cell parameters, *R* factors, goodness of fit, and profile parameters are given in Table 4. The fractional coordinates and thermal parameters for the room temperature superstructure are given in Table 5, and bond distances are listed in Table 6. The O−P−O and O−Zr−O angles do not vary by more than about 10° from their ideal values of 109° and 90°, respectively.

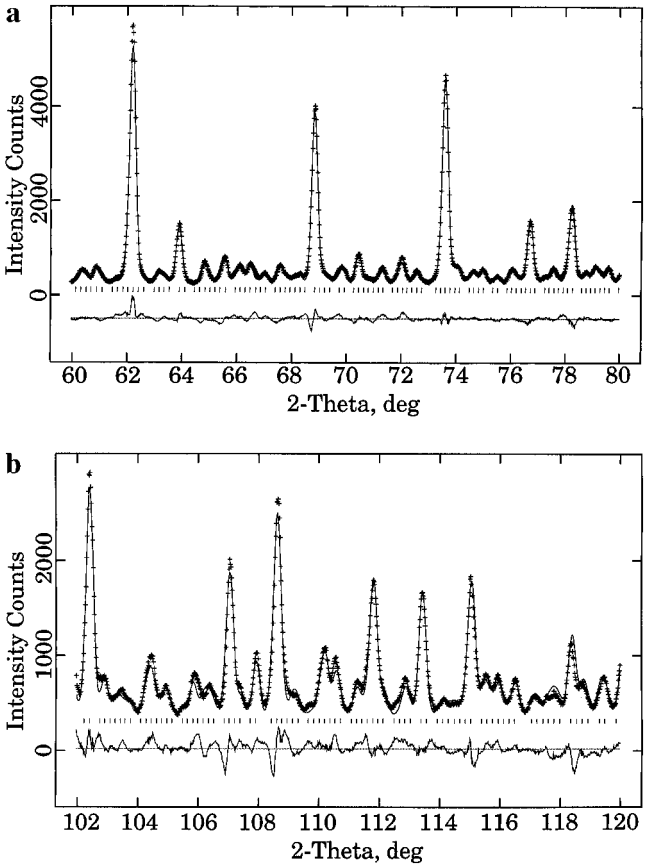

Figure 4. Observed (crosses) and calculated (line) neutron diffraction patterns for ZrP_2O_7 at 25 °C: (a) 2-θ range 60−80°. (b) 2-θ range 102−120°. Ticks indicated possible peak positions, and a difference pattern is given below.

The structure of ZrP_2O_7 at 227 °C was solved in a similar manner. Cell parameters, *R* factors, goodness of fit, and profile parameters are given in Table 4. The better goodness of fit values are misleading. This was a two-phase refinement due

(27) Larson, A. C.; Von Dreele, R. B. LANSCE MS-H805; Los Alamos National Laboratory: Los Alamos, NM, 1994.
(28) Howard, C. J. *J. Appl. Crystallogr.* **1975**, *8*, 615.
(29) Thompson, P.; Cox, D. E.; Hastings, J. B. *J. Appl. Crystallogr.* **1987**, *20*, 79.

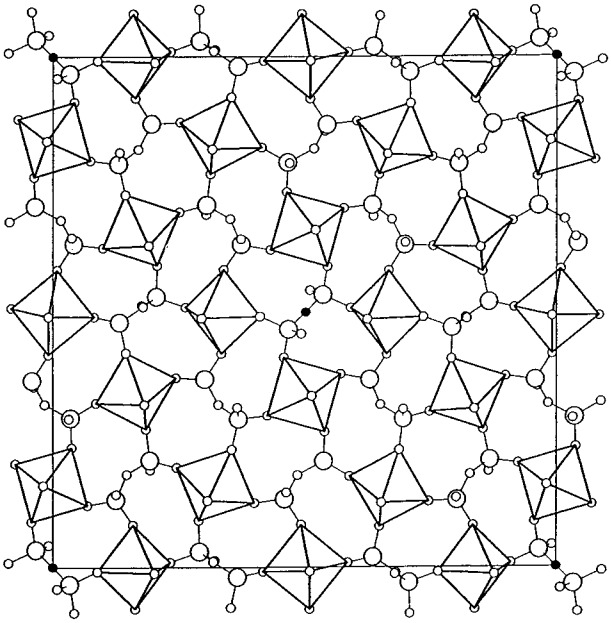

Figure 5. Section of the ZrP_2O_7 structure at 25 °C. Zirconium atoms are at the centers of the octahedra. Large open circles are phosphorus atoms. Smaller circles are oxygen atoms. All P−O−P linkages are bent except for those at the origin and face-centered positions where oxygen is shown as a filled circle.

Table 4. Cell Parameters, Agreement Factors, and Profile Parameters for Superstructure Phase

	25 °C	227 °C
a(Å)[a]	24.7424(2)	24.8026(1)
R_{wp}	0.0887	0.0642
R_{calc}	0.0632	0.0823
$R(F^2)$	0.0796	0.0932
χ^2	5.321	0.5646
U	44.2	43.8
V	−73.7	−107.2
W	147.6	125.8
A_s	17.221	13.033
$F1$	−1.092	
$F2$	−0.068	
X		5.105
S_s		−4.867

[a] Standard deviation in parentheses are those calculated by GSAS. Considering the uncertainties in the wavelength and temperature, the uncertainty of the cell edges would be much larger.

to the Al heat shields. The standard deviations of the refined positional parameters were twice as high for the data taken at 227 °C. For this reason, it is not possible to say whether or not the structure of ZrP_2O_7 changes in any significant way from 25 to 227 °C.

Discussion

The lattice symmetry of the high-temperature structure for ZrP_2O_7 forces a 180° bond angle on the P−O−P linkage. This is only the average P−O−P bond angle, and displacements of oxygen to bend the P−O−P angle either could be static and disordered or could be due to thermal motion. At higher temperatures, a distinction between these two models becomes meaningless because there would be sufficient thermal energy to facilitate the hopping of oxygen among the different sites of the static, disordered model. In any case, it is not possible on the basis of our diffraction data to distinguish between these two models. Considering the low thermal expansion of ZrP_2O_7 above 290 °C, the thermal vibration model is appealing. According to this model, increased vibration of O2 perpendicular to the P−O2−P bond would result in a decreased P−P distance. This would tend to compensate any thermal expansion of bond distances and give an overall low lattice expansion. Unfortunately, our data are not over a temperature range sufficient to test this hypothesis.

The angle for P−O−P linkages is normally in the range 130−160°. A P−O−P bond angle of 180° is unfavorable, and one expects that a structure containing such a linkage could only be stabilized by entropy at high temperature. Thus, when the cubic ZrP_2O_7 structure with $Z = 4$ is cooled, a phase transition is expected to a structure where the P−O−P bond angles bend away from 180° in an ordered, static fashion. We have previously shown that such a transition is highly frustrated in

Table 5. Fractional Coordinates and Thermal Parameters for ZrP_2O_7 at 25 °C[a]

atom	x	y	z	$U \times 100$
P(1)	0.4662	0.1309	0.1298	1.45(5)
P(2)	0.4695	0.4591	0.1300	1.45(5)
P(3)	0.7963	0.1310	0.1319	1.45(5)
P(4)	0.7967	0.7999	0.1314	1.45(5)
P(5)	0.1325	0.4637	0.8040	1.45(5)
P(6)	0.1302	0.7987	0.4649	1.45(5)
P(7)	0.4659	0.8030	0.4600	1.45(5)
P(8)	0.4687	0.7989	0.7935	1.45(5)
P(9)	0.8032	0.8032	0.8032	1.45(5)
P(10)	0.4663	0.4663	0.4663	1.45(5)
P(11)	0.1294	0.1294	0.1294	1.45(5)
Zr(1)	0.3333	0.0006	0.0054	1.31(6)
Zr(2)	0.3275	0.3355	−0.0010	1.31(6)
Zr(3)	0.9967	0.3304	0.6591	1.31(6)
Zr(4)	0.3365	0.6666	0.3349	1.31(6)
Zr(5)	0.3376	0.3376	0.3376	1.31(6)
Zr(6)	0.0000	0.0000	0.0000	1.31(6)
O(1)	0.4995	0.1474	0.1857	2.32(17)
O(2)	0.8257	0.1744	0.1655	2.32(17)
O(3)	0.5174	0.4854	0.1667	2.32(17)
O(4)	0.1867	0.4840	0.8383	2.32(17)
O(5)	0.1631	0.1631	0.1631	11.63 and −3.86[b]
O(6)	0.5000	0.5000	0.5000	20.90 and −1.80[b]
O(7)	0.1213	0.0687	0.1557	1.28(3)
O(8)	0.4751	0.0694	0.1248	1.28(3)
O(9)	0.1479	0.4115	0.1407	1.28(3)
O(10)	0.1646	0.0852	0.4862	1.28(3)
O(11)	0.4856	0.3971	0.1250	1.28(3)
O(12)	0.4799	0.0756	0.4756	1.28(3)
O(13)	0.1635	0.4213	0.4753	1.28(3)
O(14)	0.4780	0.4110	0.4889	1.28(3)
O(15)	0.8063	0.0773	0.1524	1.28(3)
O(16)	0.1340	0.7375	0.1317	1.28(3)
O(17)	0.1353	0.0740	0.8019	1.28(3)
O(18)	0.8159	0.7445	0.1452	1.28(3)
O(19)	0.8262	0.0808	0.8201	1.28(3)
O(20)	0.1502	0.7434	0.8136	1.28(3)
O(21)	0.8059	0.7463	0.8343	1.28(3)
O(22)	0.1494	0.4010	0.8007	1.28(3)
O(23)	0.1425	0.7328	0.4695	1.28(3)
O(24)	0.4880	0.7486	0.1480	1.28(3)
O(25)	0.4637	0.7455	0.4681	1.28(3)
O(26)	0.4977	0.4187	0.8282	1.28(3)
O(27)	0.4905	0.7435	0.7932	1.28(3)
O(28)	0.4780	0.0663	0.7959	1.28(3)
O(29)	0.8294	0.0802	0.4633	1.28(3)
O(30)	0.8203	0.4148	0.1509	1.28(3)
O(31)	0.7999	0.3990	0.4580	1.28(3)
O(32)	0.8187	0.4163	0.7964	1.28(3)
O(33)	0.8202	0.7332	0.4800	1.28(3)

[a] $U_{eqv} \times 100 = 11.63$ (20.90) are defined as $^1/_3$ the trace of the diagonalized matrix. The estimated standard deviations for atomic positions from GSAS are between ±0.0004 and ±0.0007 with Zr giving the lower value. [b] There are two values listed for O5 (and O6) since they are refined with anisotropic thermal parameters. $U11 = U22 = U33 = 0.1163$ (0.2090), and $U12 = U13 = U23 = -0.0386$ (−0.0180).

Table 6. Bond Distances (Å)[a] for ZrP_2O_7 at 25 °C

P1−O1	1.66	P5−O29	1.44
P1−O8	1.54	P6−O4	1.53
P1−O9	1.45	P6−O23	1.66
P1−O10	1.47	P6−O28	1.61
P2−O3	1.63	P6−O30	1.44
P2−O11	1.59	P7−O3	1.52
P2−O12	1.45	P7−O25	1.44
P2−O13	1.51	P7−O26	1.62
P3−O2	1.54	P7−O31	1.52
P3−O15	1.45	P8−O1	1.63
P3−O16	1.46	P8−O27	1.47
P3−O17	1.44	P8−O32	1.44
P4−O2	1.54	P8−O33	1.61
P4−O18	1.49	P9−O5	1.44
P4−O19	1.53	P9−O21 × 3	1.60
P4−O20	1.44	P10−O6	1.44
P5−O4	1.66	P10−O14 × 3	1.51
P5−O22	1.61	P11−O5	1.44
P5−O24	1.54	P11−O7 × 3	1.65
Zr1−O8	1.99	Zr3−O19	1.97
Zr1−O10	2.17	Zr3−O24	2.01
Zr1−O14	2.05	Zr3−O26	2.21
Zr1−O25	2.24	Zr3−O33	1.94
Zr1−O28	2.07	Zr4−O9	2.03
Zr1−O29	2.12	Zr4−O16	2.16
Zr2−O11	2.01	Zr4−O18	2.05
Zr2−O15	2.13	Zr4−O21	2.12
Zr2−O17	2.04	Zr4−O22	1.91
Zr2−O23	1.98	Zr4−O32	2.21
Zr2−O27	2.06	Zr5−O20 × 3	2.11
Zr2−O31	2.02	Zr5−O30 × 3	1.98
Zr3−O7	2.04	Zr6−O12 × 6	2.03
Zr3−O13	2.06		

[a] Estimated standard deviations from GSAS are between ±0.01 and ±0.02 Å for Zr−O distances and are between ±0.02 and ±0.03 Å for P−O distances.

this structure.[21] Even if one allows the symmetry to drop to triclinic, the connectivity of the ZrP_2O_7 lattice is such that good bond distances and angles cannot be obtained in the $Z = 4$ unit cell. Instead, a $3 \times 3 \times 3$ superstructure forms. Then 89% of the P−O−P groups are no longer on 3-fold axes, and the P−O−P bond angle of such groups can take on normal values (134−162°). For the 11% of P−O−P groups remaining on the 3-fold axes, the question remains as to whether to treat the oxygen bending the P−O−P linkage as static and disordered or as thermal motion.

Apparently only one other structure containing pyrophosphate groups has been refined where an average 180° P−O−P angle was required by lattice symmetry. This is $Mn_2P_2O_7$, where the P−O−P linkage lies on a 2-fold axis.[30] The displacements of the bridging oxygen were modeled both as a thermal ellipsoid and as a static disordered situation. The disordered model gave a slightly better fit to the data, inadequate to firmly resolve the issue. The static disordered model gave a P−O−P angle of 162−166° depending on the space group assumed and whether X-ray single crystal or neutron powder data were used. For all of our refinements of high-temperature ZrP_2O_7, we obtain a P−O−P angle of about 145° from our static disordered model and 170° on the basis of root mean square displacement of the thermal ellipsoid in the ordered model. The smaller value falls within the normal range of P−O−P angles, whereas the larger value would be considered unusually large but is not far from the value estimated for $Mn_2P_2O_7$.

Acknowledgment. The furnace used to collect the high-temperature data was constructed by Richard W. Rothe, Jr. The neutron data were collected at the high-flux beam reactor at Brookhaven National Laboratory, which is supported by the Division of Materials Sciences, U.S. Department of Energy, under Contract DE-AC02-76CH0016. This work was supported in part by NSF Grant DMR-9308530.

IC950844X

(30) Stefanidis, T.; Nord, A. G. *Acta Crystallogr*. **1984**, *40*, 1995.